Lens-Coupled Imaging Arrays for the Millimeter- and Submillimeter-Wave Regions

Kazuhiro Uehara, Kazuhito Miyashita, Ken-Ichiro Natsume, Kouki Hatakeyama, and Koji Mizuno, *Senior Member, IEEE*

Abstract—We have been developing four kinds of lens-coupled antenna imaging arrays for operation at millimeter- and submillimeter-wave frequencies. The comparison between dipole antennas, Yagi-Uda's, trap-loaded antennas, and microstrip patches will be discussed from the viewpoint of the matching with the detectors and optical systems. The radiation patterns and input impedance of each antenna have been calculated and measured to attain the optimum matching using model experiments. The trap-loaded antenna arrays have been successfully applied to plasma diagnostics at the Tsukuba GAMMA 10 tandem mirror.

I. INTRODUCTION

MILLIMETER and submillimeter wavelength imaging has recently become increasingly important in remote sensing, plasma diagnostics, radio astronomy, and environmental measurements. Accordingly the high-performance multi-element quasi-optical imaging systems have been developed [1]-[5]. The imaging systems require sensitive antennas and detectors, and high resolution optical systems. Planar antenna arrays with integrated detectors have led to improved sensitivity and scanning speed. We have investigated several kinds of printed antennas [5]-[8], which are integrated with detectors and are combined with a low-loss dielectric substrate lens. This structure eliminates RF feed cable losses and substrate modes losses [9], and offers mechanical stability and facility for cooling. On the other hand, the antennas require careful matching to the detectors and optics. In this paper, we will discuss the comparison between the lens-coupled printed antennas: dipoles, Yagi-Uda's, trap-loaded antennas and microstrip patches, all of which are integrated with beam-lead Schottky diodes. Also the measurement of plasma density profile with an imaging array at the University of Tsukuba GAMMA 10 tandem mirror will be shown as a practical application.

II. YAGI-UDA ANTENNA IMAGING ARRAYS

The fundamental configuration of the arrays consists of half-wave dipoles integrated with diodes on a dielectric-air interface [8]. The input impedance of the dipole is generally much larger than that of diodes or SIS junctions,

which causes large mismatch loss, because of difficulty to fabricate small-size matching circuits on the each array element. In addition, the dipole radiation pattern shows big sidelobes and a large central dip in the *H*-plane [10] (Fig. 2(a)). To improve the radiation patterns, we have proposed and fabricated Yagi-Uda antenna configuration [6] shown in Fig. 1. The radiator elements are photolithographically fabricated half-wave dipoles on a substrate of PTFE/glass ($\epsilon_r = 2.17$), and the SBD's are integrated at the feed point of each radiator. The director elements are on the other side of the substrate to which a hyper-hemispherical lens of 60 mm diameter, made of TPX ($\epsilon_r = 2.13$), is attached. The spacing between the radiator and the director can be controlled by choosing the substrate with proper thickness. For optimization of the antenna configuration, the element dimensions are determined by two conditions: one is impedance matching with the detector, and the other is beam pattern matching with the optical system. The radiation pattern can be adjusted by changing the director length and the element spacing.

Fig. 2(b) shows optimized Yagi-Uda patterns. The radiator length $2l_1$ is $0.5\lambda_e$, the director length $2l_2$ is $0.462\lambda_d$, and the spacing d is $0.093\lambda_d$. λ_e and λ_d are the effective wavelength at the air-dielectric interface and the wavelength in the dielectric, respectively, being defined by

$$\lambda_e = \frac{\lambda_0}{\sqrt{(1 + \epsilon_r)/2}}, \tag{1}$$

$$\lambda_d = \frac{\lambda_0}{\sqrt{\epsilon_r}}. \tag{2}$$

The improved pattern is almost symmetrical and the directivity G_d is 5.5 dB. The directivity is defined by

$$G_d = \frac{|D(0, 0)|^2}{\dfrac{1}{4\pi} \displaystyle\int |D(\theta, \phi)|^2 \, d\Omega}, \tag{3}$$

where $D(\theta, \phi)$ is the directivity function. Because the diameter of the hyperhemispherical lens is electrically large and the substrate modes can be neglected, we have applied the moment method to the dielectric half spaces to calculate current distributions on the radiator and the director [11]. The theoretical patterns have been calculated from these current distributions. The experimental pat-
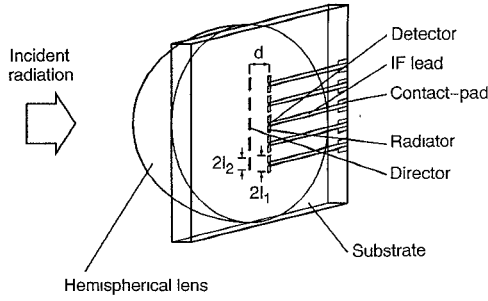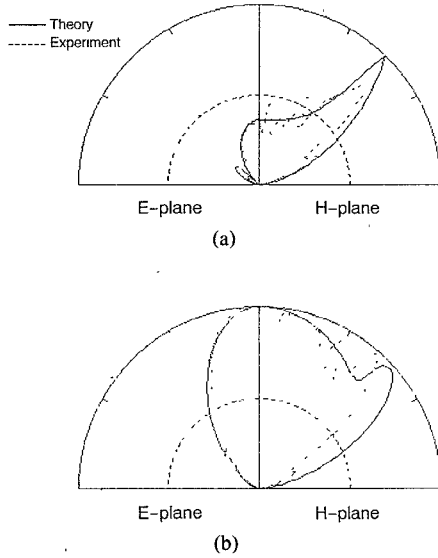
Fig. 1. Yagi-Uda antenna imaging array.

Fig. 2. The calculated and measured radiation patterns of an antenna on a dielectric hemisphere ($\epsilon_r = 2.13$) of 100 mm diameter. (a) Dipole. (b) Yagi-Uda ($2l_1 = 0.5\lambda_e$, $2l_2 = 0.462\lambda_d$, $d = 0.093\lambda_d$). The scale is linear in power; ——— theory, --- experiment at 50 GHz.
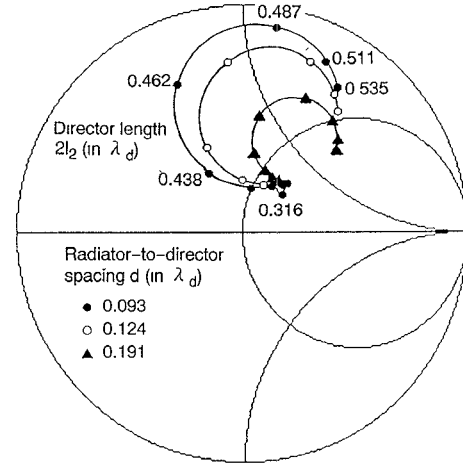

Fig. 3. The calculated input impedance of a Yagi-Uda antenna on a dielectric hemisphere ($\epsilon_r = 2.13$).
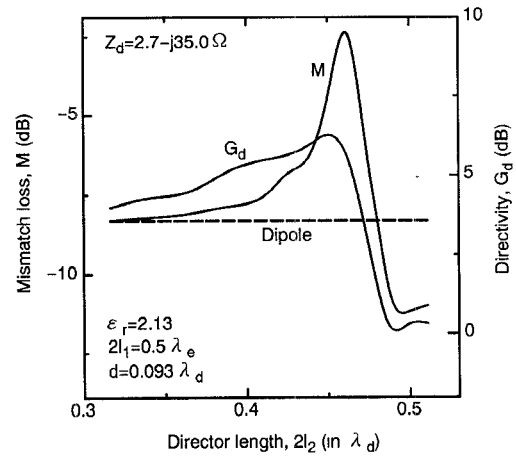

Fig. 4. The calculated directivity and mismatch loss of a Yagi-Uda antenna ($2l_1 = 0.5\lambda_e$, $d = 0.093\lambda_d$) versus director length $2l_2$. The diode impedance is $2.7 - j35.0 \ \Omega$.

terns were measured in an anechoic chamber at 50 GHz band using TPX hemispherical lens of 100 mm diameter. The results agree well with the theory although many ripples are obtained in the *H*-planes. These ripples are due to the leaky radiations from the electric fields across the parallel low-frequency leads.

The input impedance can be tuned over a broad range by adjusting the element dimensions (Fig. 3), leading to good matching conditions without complex matching circuits. The detectors are beam-lead Schottky diode (Sanyo Electric Co. Ltd., SBL-221) with typical R_s of 4.1 Ω, R_j of 540 Ω, C_j of 31 fF and C_p of 60 fF at a 50 μA bias current, with a cutoff frequency larger than 400 GHz. These parameters were estimated from the diode structure [12], and the results agree with the dc and microwave measurements with the use of Cascade probe station and the HP-8510 network analyzer in the frequency range from 1 to 18 GHz. The calculated small-signal impedance with an RF equivalent circuit at 50 GHz is $2.7 - j35.0 \ \Omega$. The SBD's are useful for imaging applications because they can be used for both video detectors and heterodyne mixers at room temperature. Fig. 4 shows calculated directivity and mismatch loss versus the director length. The mis-

match loss M between the antenna and the diode is defined by

$$M = \frac{4 \ \text{Re} \ \{Z_a\} \ \text{Re} \ \{Z_d\}}{|Z_a + Z_d|^2}, \tag{4}$$

where Z_a is the antenna input impedance and Z_d is the impedance of the diode.

Considering both the impedance mismatch and the directivity, we can estimate the total efficiency of the individual receptor. Fig. 5 shows calculated and measured total sensitivity of the receptor. For the optimized Yagi-Uda, the receiving power from an incident plane wave is theoretically improved 8 dB in comparison with the dipole only, and experimentally a 6 dB increase in power has been measured. In the collinear Yagi-Uda array, cross-talk levels of less than -20 dB between adjacent antennas have been measured when the element interval is $0.7\lambda_d$ in 5 GHz model experiments. These levels are negligible for constructing imaging arrays with the *f*-number of 1.0. A total receptor 3 dB bandwidth of 19% for the dipole and 15% for the Yagi-Uda have been measured at 50 GHz band.
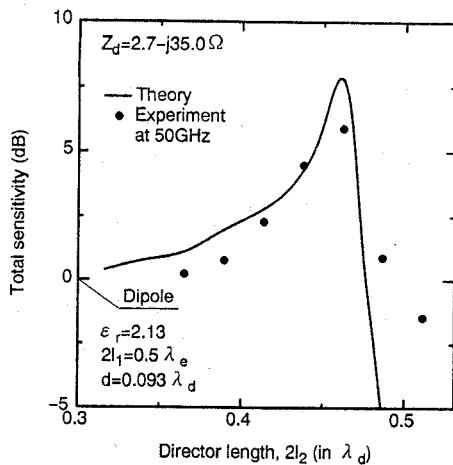
Fig. 5. Total sensitivity of a Yagi–Uda receptor versus director length $2l_2$. The 0 dB line shows the sensitivity of the dipole; —— theory, ● experiment at 50 GHz.
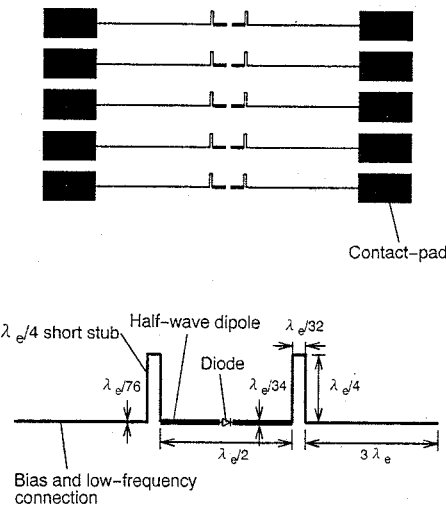

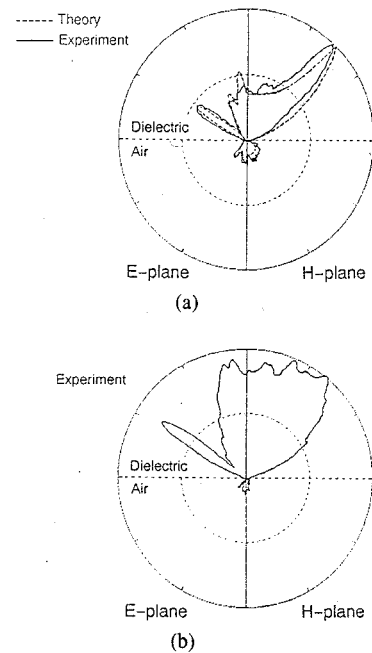Fig. 6. The configuration of a trap-loaded dipole imaging array.

Fig. 7. The calculated and measured radiation patterns of a trap-loaded antenna on a dielectric hemisphere ($\epsilon_r = 2.13$) of 100 mm diameter. (a) Dipole. (b) Yagi–Uda ($2l_1 = 0.5\lambda_e$, $2l_2 = 0.414\lambda_d$, $d = 0.124\lambda_d$). The scale is linear in power; --- theory, —— experiment at 50 GHz.

III. TRAP-LOADED ANTENNA IMAGING ARRAYS

The dipole configuration shown in Fig. 1 offers some difficulties to fabricate parallel array because of the obstruction of the bias and low-frequency leads. In order to avoid any complex circuit designs which might degrade radiation patterns or crosstalks, we have designed trap-loaded antenna configuration [13] shown in Fig. 6. In this structure, the leads are taken from the edges of the dipole through high impedance traps. Each trap consists of a quarter-wavelength long short-stub which offers a high Q-value.

Fig. 7 shows measured radiation patterns for the trap-loaded dipole (a) and the Yagi–Uda configuration (b) with $2l_2$ of $0.414\lambda_d$ and d of $0.124\lambda_d$. Fig. 7(a) also shows dipole patterns calculated by assuming sinusoidal standing waves which have large amplitude on the dipole, and small amplitude on the $3\lambda_e$ long outer sections. Undesirable radiations from the waves on the outer sections degrade radiation patterns and cause larger sidelobes in the E-plane. The directivity of 3.7 dB for the dipole and 5.9

dB for the optimized Yagi–Uda have been measured at 50 GHz experiment. The cross-polarization pattern level of the trap-loaded dipole have been measured to be less than −20 dB at $\phi = 45°$, which indicates that the troublesome radiations from the traps might be small. The antenna input impedances become higher than the previous structures due to the effects of the outer sections. The impedance of the dipole with $2\lambda_e$ long traps have been measured to be about 200 Ω using 5 GHz model experiment. Hence these antennas might be useful for heterodyne detection because the RF impedance of the pumped diode is much larger than the small signal impedance [14]. A total receptor 3 dB bandwidth of 10% and 8% were measured at 50 GHz for the dipole and Yagi–Uda antenna, respectively. The results show narrower bandwidths than the previous structure because of the additional high Q-value traps.

IV. PATCH ANTENNA IMAGING ARRAYS

Although the Yagi–Uda configurations have offered good performance and a simple structure for easy fabrication, lack of efficient space is one of the disadvantages for constructing additional integrated circuits. This is particularly important in fabricating two-dimensional arrays [1]. Therefore, we have proposed a lens-coupled patch antenna imaging array configuration which is very suitable for fabricating two-dimensional arrays using MMIC technique (Fig. 8). This array consists of two individual microstrip substrates separated by a common metal ground plane. The antennas are printed on the first substrate (ϵ_{r2}) covered with the low-loss dielectric lens (ϵ_{r1}). Each antenna is fed with a via-hole or coupling slot [15], [16]
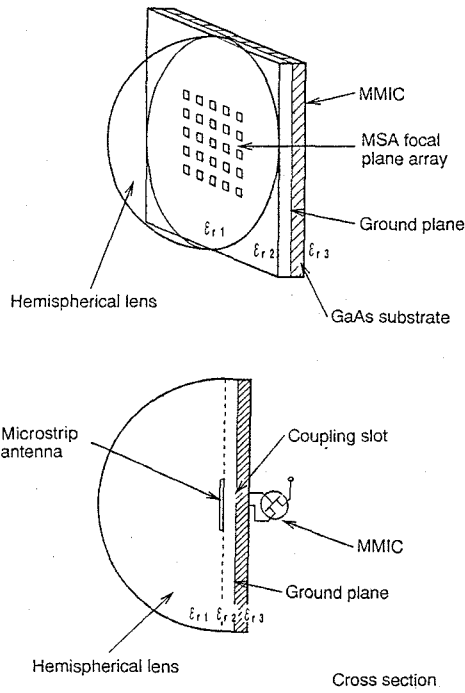
Fig. 8. The configuration of a two-dimensional microstrip patch antenna imaging array.

Fig. 9. The calculated radiation patterns of a microstrip patch antenna on a dielectric hemisphere for various ϵ_{12}, where ϵ_{12} is the ratio of the dielectric constant of the substrate (ϵ_{r2}) to the lens (ϵ_{r1}). The scale is linear in power.

Fig. 10. The calculated and measured two-dimensional radiation patterns of a microstrip patch antenna on a dielectric hemisphere of 100 mm diameter ($\epsilon_{r1} = \epsilon_{r2} = 2.13$). (a) Theory. (b) Experiment at 52 GHz. The scale is linear in power.

from the MMIC constructed on the second substrate (ϵ_{r3}). The second substrate offers an efficient space for fabricating additional integrated circuits such as matching circuits, mixers, amplifiers, and interconnections. The antennas are ideally isolated from these circuits by the ground plane.

Fig. 9 shows calculated radiation patterns of the individual antenna [17] versus ϵ_{12}:

$$\epsilon_{12} \equiv \frac{\epsilon_{r2}}{\epsilon_{r1}}, \tag{5}$$

which is defined by the ratio of the dielectric constant of the first substrate ϵ_{r2} to the dielectric constant of the lens ϵ_{r1}. Both the patch length a and the patch width b are

$$a = b = \frac{\lambda_{eff}}{2}, \tag{6}$$

where the effective wavelength in the first substrate λ_{eff} is defined by

$$\lambda_{eff} = \frac{\lambda_0}{\sqrt{\epsilon_{r2eff}}}, \tag{7}$$

and the effective dielectric constant of the first substrate ϵ_{r2eff} is given by

$$\epsilon_{r2eff} = \frac{\epsilon_{12} + 1}{2} + \frac{\epsilon_{12} - 1}{2}\left(1 + \frac{10h_2}{b}\right)^{-1/2}, \tag{8}$$

where h_2 is the thickness of the first substrate, and b is the patch width [18]. If ϵ_{r1} equals ϵ_{r2} then the ratio ϵ_{12} becomes one, and then an ideal radiation pattern which is almost symmetrical for both the E- and H-planes can be realized. This pattern has neither any sidelobes nor trou-
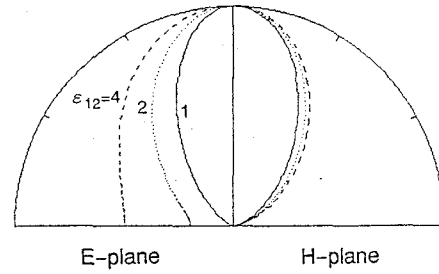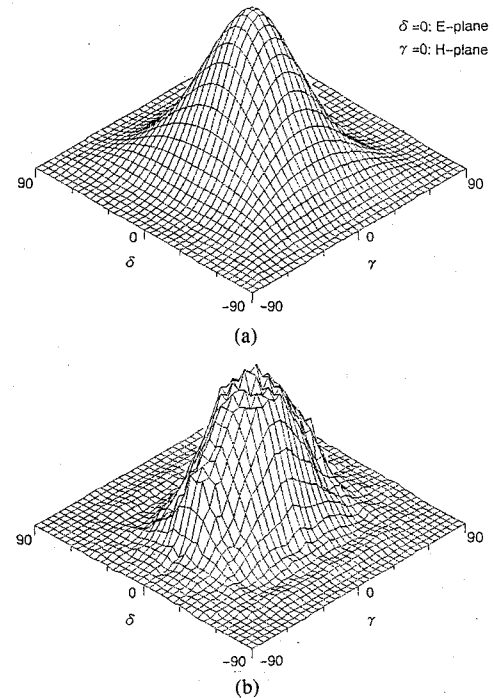
blesome radiations at the horizontal directions, which offers low crosstalk and high beam coupling efficiency to the incident beam. When ϵ_{12} does not equal one, a troublesome substrate mode occurs in the first substrate which affects the radiation and impedance characteristics of the adjacent antennas in the array [19]. The affected patterns accordingly disagree with those shown in Fig. 9. Fig. 10 shows calculated (a) and measured (b) two-dimensional radiation pattern for $\epsilon_{12} = 1$ at 52 GHz using a TPX hemispherical lens of 100 mm diameter in an anechoic chamber. The feed point (x_0, y_0) is $(0.25a, 0.5b)$ in our configuration. The results agree well with theory: the calculated directivity is 9.8 dB and the 3 dB beamwidths are 60° in the E-plane and 71° in the H-plane.

The antenna input impedance of $79 + j24 \ \Omega$ has been calculated with a cavity model [20], and $83 + j25 \ \Omega$ was measured at 6 GHz model experiments using polyethylene
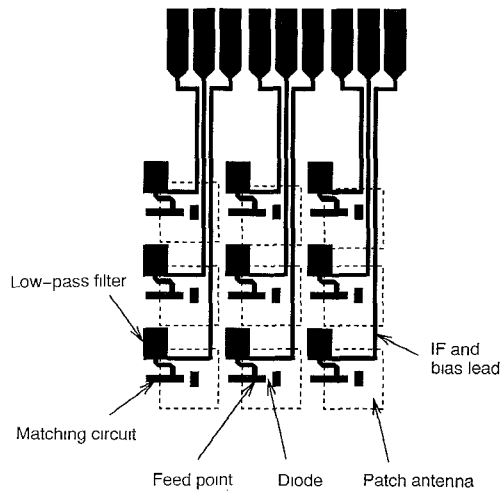
Fig. 11. The configuration of 3 × 3 monolithic microstrip patch antenna imaging array (bottom view).
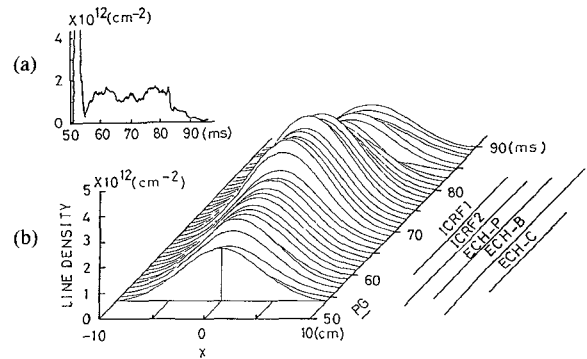

Fig. 12. The measurement of the time evolutions of the line-density (a) and line-density profile (b) at the plug cell in the Tsukuba GAMMA 10 plasma with a 10 element trap-loaded Yagi–Uda antenna imaging array at 70 GHz. The time sequence is as follows: following the gun-produced plasma injection (PG), the plasma is heated with ion cyclotron range of frequency (ICRF) powers and electron cyclotron heating (ECH) powers.

substrates ($\epsilon_{r1} = \epsilon_{r2} = 2.28$). A crosstalk level of less than -20 dB in both the E- and H-planes when the element spacing is $0.7\lambda_d$ has been measured at the experiments. Fig. 11 shows an example of the configuration of our 3 × 3 integrated patch array. The squares of dot-line show the patch antennas arrayed by the spacing of $0.7\lambda_d$. Matching circuits and low-pass filters are fabricated behind each unit. Since we can construct matching circuits in the second microstrip substrate, the mismatch loss between the antenna and a detector element can be minimized. Consequently this configuration is suitable for various kinds of detectors. The total 3 dB bandwidth of 6% have been measured at 50 GHz using the TPX lens and Schottky diode detectors.

V. APPLICATIONS

As a practical application of our imaging array, we have applied a 10 element trap-loaded parallel Yagi–Uda array to the University of Tsukuba GAMMA 10 tandem mirror in order to measure the plasma density profile, for which we have constructed a 70 GHz heterodyne phase imaging system [21]. The IF frequency used is 500 kHz. The optical system has been designed and estimated by using a ray-tracing code as well as a Gaussian-beam propagation theory [22]. The substrate lens is made of fused quartz ($\epsilon_r = 4$), producing a magnification of 4.0, and other lenses for 70 GHz optics are made with low-density polyethylene ($\epsilon_r = 2.28$), yielding a magnification of 4.3. The system f-number of 1.0 determines the cutoff spatial frequency f_0^E of $233m^{-1}$ and the diffraction-limited sampling interval T_E of 2.14 mm ($1.0\lambda_d$) by

$$f_0^E = \frac{n}{2\lambda_0 f\text{-number}}, \qquad (9)$$

$$T_E = \frac{1}{2f_0^E}, \qquad (10)$$

where n is the index of refraction of the substrate lens [23]. The sampling interval corresponds to a plasma dimension of 37 mm. The image can be reconstructed by the Whittaker–Shannon sampling theorem [24]. The sys-

tem has been tested to provide diffraction-limited phase images using dielectric targets by the same method as Young *et al.* [25]. Fig. 12 shows time evolutions of the line-density (a) and line-density profile (b) at the plug cell. The initial plasma produced by a plasma gun cannot be measured since the density is above the cut-off. The results are very close to those obtained by a millimeter-wave interferometer with scanning horn antennas, which is used for the cross-calibration.

VI. CONCLUSION

We have designed and investigated several kinds of lens-coupled antennas for operation at millimeter and submillimeter wavelength. The Yagi–Uda antennas have been successfully used with improved radiation patterns as well as impedance mismatch loss for small impedance detectors. Trap-loaded antennas were also designed in parallel arrays and successfully applied for plasma diagnostic experiments at 70 GHz. The lens-coupled patch antennas showed good radiation patterns and the stacked microstrip configuration has made possible the fabrication of multifunction monolithic arrays.
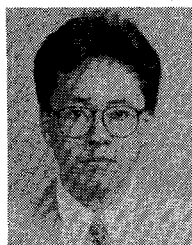
REFERENCES

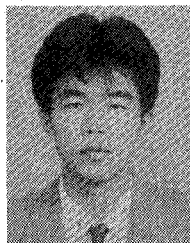[1] G. M. Rebeiz, D. P. Kasilingam, Y. Guo, P. A. Stimson, and D. B. Rutledge, "Monolithic millimeter-wave two-dimensional horn imaging arrays," *IEEE Trans. Antennas Propagat.*, vol. 38, pp. 1473–1482, Sept. 1990.
[2] P. H. Siegel and R. J. Dengler, "The dielectric-filled parabola: a new millimeter/submillimeter wavelength receiver/transmitter front end," *IEEE Trans. Antennas Propagat.*, vol. 39, pp. 40–47, Jan. 1991.

[3] W. Chew and H. R. Fetterman, "Printed circuit antennas with integrated FET detectors for millimeter-wave quasi optics," IEEE Trans. Microwave Theory Tech., vol. 37, pp. 593-597, Mar. 1989.

[4] K. S. Yngvesson, T. L. Korzeniowski, Y. Kim, E. L. Kollberg, and J. F. Johansson, "The tapered slot antenna—a new integrated element for millimeter-wave applications," IEEE Trans. Microwave Theory Tech., vol. 37, pp. 365-374, Feb. 1989.

[5] K. Uehara, T. Yonekura, H. Nishimura, K. Miyashita, and K. Mizuno, "Millimeter-wave Yagi-Uda antenna imaging arrays," in Proc. 3rd Asia-Pacific Microwave Conf., 1990, pp. 365-368.

[6] K. Mizuno, K. Uehara, H. Nishimura, T. Yonekura, and T. Suzuki, "Yagi-Uda array for millimeter-wave imaging," Electron. Lett., vol. 27, no. 2, pp. 108-109, Jan. 1991.

[7] Y. Daiku, K. Mizuno, and S. Ono, "Dielectric plate antenna for monolithic Schottky-diode detectors," Infrared Physics, vol. 18, pp. 697-682, 1978.

[8] K. Mizuno, Y. Daiku, and S. Ono, "Design of printed resonant antennas for monolithic-diode detectors," IEEE Trans. Microwave Theory Tech., vol. MTT-25, pp. 470-472, June 1977.

[9] D. B. Rutledge and M. S. Muha, "Imaging antenna arrays," IEEE Trans. Antennas Propagat., vol. AP-30, pp. 535-540, July 1982.

[10] C. R. Brewitt-Taylor, D. J. Gunton, and H. D. Rees, "Planar antennas on a dielectric surface," Electron. Lett., vol. 17, no. 20, pp. 729-730, Oct. 1981.

[11] T. Mashiko, Y. He, T. Uno, and S. Adachi, "The transient fields of a dipole antenna located near the interface of lossy half-space," Proc. ISAP, vol. 3C4-3, pp. 731-734, 1989.

[12] Y. Harada and H. Fukuda, "A novel beam lead GaAs Schottky-barrier diode fabricated by using thick polyimide film," IEEE Trans. Electron. Devices, vol. ED-26, pp. 1799-1804, Nov. 1979.

[13] J. G. Heston, S. M. Wentworth, R. L. Rogers, D. P. Neikirk, and T. Itoh, "MM wave/FIR twin slot antenna structures," in IEEE Antennas Propagat. Soc. Int. Symp. Dig., vol. 2, May 1990, pp. 788-790.

[14] S. A. Maas, Microwave Mixers. Dedham, MA: Artech House, 1986.

[15] D. M. Pozar, "Five novel feeding techniques for microstrip antennas," in IEEE Antennas Propagat. Soc. Int. Symp. Dig., June 1987, pp. 920-923.

[16] M. I. Aksun, S. Chuang, and Y. T. Lo, "On slot-coupled microstrip antennas and their applications to CP operation-theory and experiment," IEEE Trans. Antennas Propagat., vol. 38, pp. 1224-1230, Aug. 1990.

[17] J. R. James, P. S. Hall, and C. Wood, Microstrip Antenna Theory and Design, ch. 4. London: Peregrinus, 1981.

[18] M. V. Schneider, "Microstrip lines for microwave integrated circuits," Bell System Tech. J., vol. 48, pp. 1421-1444, May/June 1969.

[19] A. K. Bhattacharyya, "Characteristics of space and surface waves in a multilayered structure," IEEE Trans. Antennas Propagat., vol. 38, pp. 1231-1238, Aug. 1990.

[20] Y. T. Lo, D. Solomon, and W. F. Richards, "Theory and experiment on microstrip antennas," IEEE Trans. Antennas Propagat., vol. AP-27, pp. 137-145, Mar. 1979.

[21] K. Hattori, A. Mase, A. Itakura, M. Inutake, S. Miyoshi, K. Uehara, T. Yonekura, H. Nishimura, K. Miyashita, and K. Mizuno, "Millimeter-wave phase-imaging interferometer for the GAMMA 10 tandem mirror," Rev. Sci. Instrum., vol. 62, pp. 2857-2861, Dec. 1991.

[22] H. Kogelnik and T. Li, "Laser beams and Resonators," Proc. IEEE, vol. 54, pp. 1312-1329, Oct. 1966.

[23] D. B. Rutledge, D. P. Neikirk, and D. P. Kasilingam, "Integrated-circuit antennas," in Infrared and Millimeter Waves, vol. 10, K. J. Button Ed. New York: Academic, 1983, pp. 63-86.

[24] J. W. Goodman, Introduction to Fourier Optics. New York: McGraw-Hill, 1968.

[25] P. E. Young, D. P. Neikirk, P. P. Tong, D. B. Rutledge, and N. C. Luhmann, "Multichannel far-infrared phase imaging for fusion plasmas," Rev. Sci. Instrum., vol. 56, pp. 81-89, Jan. 1985.

Kazuhiro Uehara was born in Tokyo, Japan, on April 30, 1963. He received the B.E. and M.E. degrees in electronic engineering from Tohoku University, Sendai, Japan, in 1987 and 1989, respectively. He is currently enrolled in the D.E. degree program in electronic engineering at the Research Institute of Electrical Communication of Tohoku University, Sendai, Japan. His interests include millimeter- and submillimeter-wave integrated array antennas, radiometers, and imaging/radar systems.

He is a Fellow of the Japan Society for the Promotion of Science for Japanese Junior Scientists, and he is a member of the Institute of Electronics, Information and Communication Engineers of Japan.

Kazuhito Miyashita was born in Yamanashi, Japan, on May 27, 1967. He received the B.E. and M.E. degrees in electronic engineering from Tohoku University, Sendai, Japan in 1989 and 1991, respectively.

He developed millimeter-wave integrated patch antenna imaging arrays at the Research Institute of Electrical Communications of Tohoku University. In 1991, he joined the Microwave and Optical Equipment Department, Kamakura Works of Mitsubishi Electric Corporation, Kanagawa, Japan.
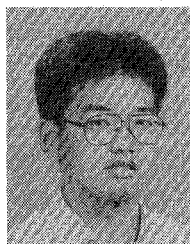
Mr. Miyashita is a member of the Institute of Electronics, Information and Communication Engineers of Japan.

Ken-Ichiro Natsume was born in Nagoya, Japan, on March 5, 1968. He received the B.E. degree from Tohoku University, Sendai, Japan in 1990. Currently, he is working for the M.E. degree in the field of millimeter- and submillimeter-wave semiconductor devices and integrated antennas at Research Institute of Electrical Communication of Tohoku University.

He was involved in R&D work concerned with telecommunication networks at TFL (Telecommunication Research Laboratory) in Horsholm, Denmark, in 1990.

Kouki Hatakeyama was born in Akita, Japan, on December 14, 1968. He received the B.E. degree in electronic engineering from Tohoku University, Sendai, Japan, in 1991.

He has developed millimeter-wave imaging arrays at the Research Institute of Electrical Communication of Tohoku University.

Koji Mizuno (M'72-SM'72) was born in Sapporo, Hokkaido, Japan on July 17, 1940. He received the B.Eng., M.Eng., and D.Eng. degrees in electronic engineering from Tohoku University, Sendai, in 1963, 1965 and 1968, respectively.

In 1968, he joined the Department of Electronic Engineering, Faculty of Engineering, Tohoku University. He was appointed Associate Professor at Research Institute of Electrical Communication, Tohoku University in 1972, and since 1984 he has been a Professor of Electron Devices there. He spent a one-year sabbatical leave at Queen Mary College, University of London under the sponsorship of SRC (Science Research Council, United Kingdom) in 1973, and in 1990 spent a six-month sabbatical leave at California Institute of Technology, Pasadena and Queen Mary and Westfield College, London under the sponsorship of Monbusho (Ministry of Education, Science and Culture, Japan). He has been interested in the millimeter and submillimeter wave region of the electromagnetic wave spectrum, and his current work is in detection, generation and their applications in the region.

Dr. Mizuno is a member of the Institute of Electronics, Information and Communication Engineers, the Institute of Electrical Engineers of Japan, the Japan Society of Applied Physics, and the Japan Society of Infrared Science and Technology. In 1984 he received the 17th Kagaku Keisoku Shinoko Kai (Scientific Measurement) award. In 1990 he became a team leader of the Photodynamics Research Center, Sendai and is now running a laboratory for submillimeter wave research there as well as a laboratory in Tohoku University.